Ultrastable Super-Tonks-Girardeau Gases under Weak Dipolar Interactions

Yu Chen[1,2] and Xiaoling Cui[1,*]
[1]Beijing National Laboratory for Condensed Matter Physics, Institute of Physics, Chinese Academy of Sciences, Beijing 100190, China
[2]School of Physical Sciences, University of Chinese Academy of Sciences, Beijing 100049, China

(Received 24 April 2023; revised 1 September 2023; accepted 26 October 2023; published 14 November 2023)

The highly excited super-Tonks-Girardeau (sTG) gas was recently observed to be extremely stable in the presence of a weak dipolar repulsion. Here we reveal the underlying reason for this mysterious phenomenon. By exactly solving the trapped small clusters with both contact and dipolar interactions, we show that the reason lies in the distinct spectral responses between sTG gas and its decaying channel (bound state) when a weak dipolar interaction is present. Specifically, a tiny dipolar force can produce a visible energy shift for the localized bound state, but can hardly affect the extended sTG branch. As a result, the avoided level crossing between two branches is greatly modified in both location and width in the parameter axis of coupling strength, leading to a more (less) stable sTG gas for a repulsive (attractive) dipolar force. These results, consistent with experimental observations, are found to robustly apply to both bosonic and fermionic systems.

DOI: 10.1103/PhysRevLett.131.203002

The super-Tonks-Girardeau (sTG) state stays in a highly excited branch in one dimension (1D) under interparticle attractions, which hosts an even stronger correlation than the Tonks-Girardeau (TG) regime with hard-core repulsions. Such an intriguing state was first predicted in identical bosons by quantum Monte Carlo [1] and Bethe-ansatz methods [2], and subsequently realized in a quasi-1D ultracold Bose gas as tuning the 1D coupling strength across resonance [3]. Later, the sTG state of spin-1/2 fermions was also discovered with Bethe-ansatz solutions [4] and observed experimentally in trapped small clusters [5,6]. Recently the fermionic sTG gas has attracted great interests in exploring the itinerant ferromagnetism in 1D and various spin chain configurations without lattice [7–15].

However, the sTG gas is not always stable in practice—as moving away from resonance, the gas will eventually collapse to low-lying bound states at intermediate attraction strength, making it impossible to approach stronger correlations with higher repulsive energies. Surprisingly, such instability has recently been rescued in experiment just by adding a weak dipolar repulsion among the atoms [16]. There, the gaseous repulsive branch was shown to be extremely stable over the whole sTG regime, and can even evolve adiabatically for two rounds of interaction cycles with continuously increasing energies, realizing the quantum holonomy ever in a physical system [17]. On the other hand, when switching to a weak dipolar attraction, the sTG gas was found to be less stable instead. These observations raise two big puzzles. First, how could a weak dipolar force, which barely changes the energy of the sTG gas, influence its stability so significantly? Second, why does this influence depend on the sign of dipolar force? Up to date no definitive answers arise to these puzzles.

In this Letter, we attempt to resolve these puzzles by exactly solving three trapped atoms (bosons or spin-1/2 fermions) with both contact and dipolar interactions. Such a three-body system comprises the minimal yet fundamental model to describe the instability of the sTG branch, as manifested by its avoided level crossings with many excited bound states when tuning the coupling strength. Based on this, we show that the modified stability of the sTG gas originates from its distinct spectral response to a weak dipolar interaction, as compared with all bound state channels it decays into. Specifically, given the form of dipolar interaction as $V_{dd} \sim 1/r^3$ (r is the interparticle distance), it can accumulate much more interaction energy for the localized bound states than the extended sTG gas. As a result, as illustrated in Fig. 1, the avoided level crossing between the two branches would shift to strong attraction regime if V_{dd} is repulsive, leading to a smaller wave function overlap and thus a narrower width at their crossing. This enhances the stability of the sTG gas. Alternatively, when switching to an attractive V_{dd}, the interbranch crossing moves to the weak attraction side with a broader width, giving a less stable sTG gas. These effects, consistent with experimental observations [16], are universally applicable to identical bosons and spin-1/2 fermions. Our results suggest a powerful tool in general to tune the stability of the target state by artificially manipulating its decay channels.

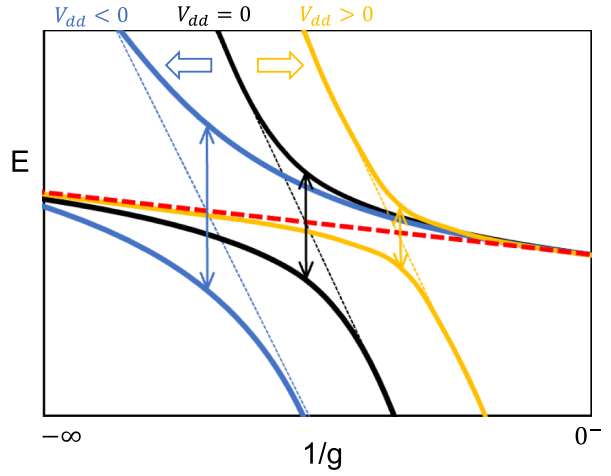

FIG. 1. Illustration for the modified stability of the sTG gas by dipolar interaction V_{dd}. Red dashed line marks the energy level of the sTG gas, which can become unstable due to the hybridization with an excited bound state (EBS, dotted line) at their avoided level crossing. In the presence of a weak V_{dd}, the sTG gas is hardly affected in energy while the EBS spectrum can be shifted visibly due to its localized wave function and large response to $V_{dd}(\sim 1/r^3)$. For a repulsive $V_{dd}(>0)$, the EBS energy is up-shifted and the avoided crossing moves to $1/g \to 0^-$ with a narrower width, giving rise to a more stable sTG gas with weaker hybridization with EBS. In comparison, an attractive $V_{dd}(<0)$ leads to a down-shifted EBS level and thus the avoided crossing moves to $1/g \to -\infty$ with a broader width (stronger hybridization), giving a less stable sTG gas.

We consider the following Hamiltonian ($\hbar = 1$):

$$H = \sum_i \left(-\frac{1}{2m}\frac{\partial^2}{\partial x_i^2} + \frac{1}{2} m\omega^2 x_i^2 \right) + \sum_{\langle i,j \rangle} \Big(g\delta(x_i - x_j) + V_{dd}(x_i - x_j) \Big); \quad (1)$$

here x_i is the 1D coordinate; ω is the harmonic trap frequency, and the trap length is defined as $l = 1/\sqrt{\mu\omega}$ ($\mu = m/2$ is the reduced mass); $g = -1/(\mu a)$ is the contact coupling with 1D scattering length a; for the dipolar interaction $V_{dd}(r)$, since its short-range part is greatly modified by higher transverse modes in realistic quasi-1D geometry [18–20]. Here we take a short-range cutoff $r_c(= 0.15l)$ and simplify it as $D/|r|^3$ for $r > r_c$ and 0 otherwise.

The three-body problem of identical bosons or spin-1/2 fermions can be exactly solved based on (1). To facilitate later discussions, we shall mainly focus on the fermion case ($\downarrow\uparrow\uparrow$) where analytical results are available. Consider a spin-$\downarrow$ atom at x_1 and two $\uparrow$ atoms at x_2, x_3; we define $r = x_2 - x_1$ and $\rho = (2/\sqrt{3})(x_3 - (x_1 + x_2)/2)$ to describe the relative motions, respectively, within a $\downarrow$-$\uparrow$ dimer and between the dimer and the rest fermion. Another set of relative coordinates $\{r_+, \rho_+\}$ can be accordingly defined by exchanging $x_2 \leftrightarrow x_3$. We then expand the three-body ansatz in the center-of-mass (c.m.) frame as $\Psi(r,\rho) = \sum_{mn} c_{mn}\phi_m(r)\phi_n(\rho)$, where ϕ_m and ϕ_n are single particle eigenstates along r and ρ with eigenenergies $\epsilon_k = (k + 1/2)\omega$ ($k = m,\ n$). Utilizing the Schrödinger equation $H\Psi(r,\rho) = E\Psi(r,\rho)$ and ensuring the fermion antisymmetry $\Psi(r,\rho) = -\Psi(r_+,\rho_+)$, we obtain the following equation for $\{c_{mn}\}$ [21]:

$$(E - \epsilon_m - \epsilon_n)c_{mn} = g\sum_{ij} c_{ij}\phi_i(0)\Big(\phi_m(0)\delta_{j,n} - A_{mn,j}\Big) + D\sum_{ij} c_{ij}\Big(B_{m,i}\delta_{j,n} - B^+_{mn,ij} + B^-_{mn,ij}\Big), \quad (2)$$

with $A_{mn,j} = \int d\rho \phi_m(\sqrt{3}\rho/2)\phi_n(-\rho/2)\phi_j(\rho)$; $B_{m,i} = \int_{|r|>r_c} dr \phi_m(r)\phi_i(r)/|r|^3$; $B^+_{mn,ij} = \int_{|r_+|>r_c} dr d\rho \phi_m(r)\phi_n(\rho)\phi_i(r_+)\phi_j(\rho_+)/|r_+|^3$; $B^-_{mn,ij} = \int_{|r_-|>r_c} dr d\rho \phi_m(r)\phi_n(\rho)[\phi_i(r)\phi_j(\rho) - \phi_i(r_+)\phi_j(\rho_+)]/(2|r_-|^3)$ (here $r_\pm = \pm r/2 + \sqrt{3}\rho/2$, $\rho_\pm = \pm\sqrt{3}r/2 - \rho/2$). Both E and $\{c_{mn}\}$ can be solved from the matrix equation (2). Similarly, the exact solutions of three identical bosons can also be obtained [21].

The trapped three-body system comprises the minimal yet fundamental model to describe the instability of the sTG gas. To see this, let us start from three fermions without dipolar interaction ($D = 0$). Their spectrum has been studied previously [7,8,10,22,23], and here we shall focus on the avoided level crossing of the sTG branch with a sequence of excited bound states, as labeled by $n = 1, 2, 3\ldots$ in Fig. 2(a) from weak to strong coupling regime. Near $1/g \to 0^-$, these bound states are essentially composed of a tight $\uparrow\downarrow$ dimer plus a free $\uparrow$ atom at excited levels, as described by the atom-dimer wave function,

$$\psi^{(m)}_{ad} = \Phi_d(r)\phi_m(\rho) - (x_2 \leftrightarrow x_3), \quad (3)$$

with energy

$$E^{(m)}_{ad} = E_d + \epsilon_m. \quad (4)$$

Here Φ_d is the dimer wave function with energy E_d, and ϕ_m is the free fermion state with energy ϵ_m. On the other hand, for the repulsive sTG branch near resonance, one can treat $1/g$ as a small parameter and construct an effective spin-chain model $H = 1/g\sum_i J_i(\mathbf{s}_i\mathbf{s}_{i+1} - 1/4)$ [11–15]. Here for three atoms the spin-exchange amplitude $J_i \equiv J$ is site independent. This gives the wave function and energy of the sTG gas as

$$\Psi_{sTG} = \Psi_0 - \frac{1}{g}\Psi_1; \quad (5)$$

$$E_{sTG} = E_0 - \frac{3J}{2g}, \tag{6}$$

where Ψ_0 is the fermionalized wave function in the hard-core limit with total energy E_0, and Ψ_1 is from the first order correction when a ↑-↓ pair comes close together [21]. For later comparisons, we have transformed Eqs. (5) and (6) into the c.m. frame [21]. Figure 2(b) shows that Eqs. (3) and (5) can indeed well approximate the two branches far from their level crossings.

Importantly, Eqs. (3) and (5) suggest qualitatively different real-space distributions between sTG and atom-dimer states. To be concrete, all atom-dimer states have a dominant weight when one ↑-↓ pair comes close to each other, i.e., $r \to 0$ or $r_+ = (r + \sqrt{3}\rho)/2 \to 0$, given that they contain very localized dimer components. In contrast, the sTG state is dominated by the Ψ_0 part which is much more extended in real space, while it only has a little weight along the dimer lines ($\sim\Psi_1/g$). Such difference is numerically confirmed in Figs. 2(c1) and 2(c3), where we have plotted real-space Ψ for different branches and the results are consistent with theoretical predictions from Eqs. (3) and (5) shown in Figs. 2(d1) and 2(d3).

The above wave-function analyses are crucial for understanding the loss mechanism of the sTG gas. As shown in Fig. 2(b), at certain g_c when the sTG state and one atom-dimer branch have perfect energy match, they can hybridize strongly and open an energy gap. Accordingly, an avoided level crossing is generated near g_c, and the resulted eigenstate inherits all the key features from both branches [Fig. 2(c2)]. Therefore, when driving the sTG gas to $\sim g_c$, it tends to develop a visible atom-dimer feature and accumulate great possibilities when ↑-↓ come close together. This leads to the instability of the sTG gas, since it can easily undergo an inelastic decay to deep molecules and cause atom loss. Similar inelastic loss due to couplings to excited molecular states was also found previously for two atoms in anharmonic potentials [24–26].

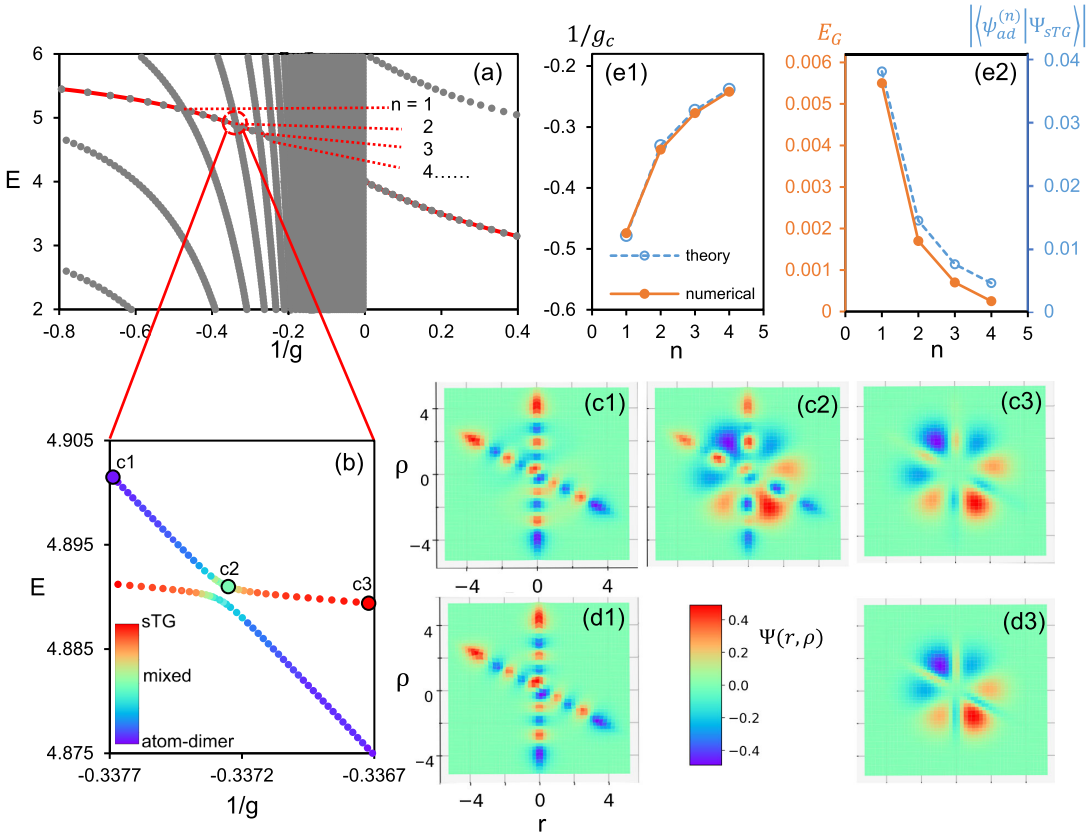

FIG. 2. Hybridization between the sTG branch and excited bound states for three harmonically trapped fermions (↑↑↓) without dipolar interaction. (a) Spectrum in the center-of-mass frame, with the lowest repulsive branch highlighted in red (the part at $1/g < 0$ is the sTG gas). Indices "$n = 1, 2, 3\ldots$" mark the locations of the avoided level crossing between sTG and various excited atom-dimer states from weak to strong couplings. (b) Magnified spectrum near the second avoided crossing ($n = 2$). The RGB color map is provided according to the wave function overlap with sTG [Eq. (5), red] and atom-dimer [Eq. (3), blue] states. (c1)–(c3) Contour plots of normalized $\Psi(r, \rho)$ for three typical coupling strengths as marked in (b). For comparison, (d1),(d3) show theoretical predictions to (c1), (c3) based on Eqs. (3) and (5). (e1),(e2) show the location $1/g_c$ and energy gap E_G for each avoided level crossing. For comparison, the theoretical prediction to $1/g_c$ by comparing (4) and (6) is shown in (e1), and the wave function overlap between (3) and (5) is shown in (e2). In all plots we take ω and l as the units of energy (E) and length (r, ρ). The units of g and Ψ are, respectively, ωl and l^{-1}.

Practically, the loss possibility of the sTG gas depends on how strongly it couples to the excited bound states, which can be evaluated by the energy gap E_G at each avoided crossing. Numerically, E_G can be extracted as the minimal energy difference at each avoided crossing, and accordingly the location g_c can also be identified, as shown in Figs. 2(e1) and 2(e2). We can see that as the crossing point moves away from resonance (smaller "n"), E_G becomes larger, consistent with a larger wave function overlap between ψ_{sTG} and $\psi_{ad}^{(n)}$ [see comparison in Fig. 2(e2)]. This indicates a less stable sTG gas, since it has a stronger hybridization with excited bound states in a broader interaction window and thus can easily transit to decay channels. Such picture is supported by experimental observations that the sTG gas eventually collapses at intermediate $g(<0)$ when moving away from resonance [3,16].

Given the loss mechanism of the sTG gas as above, now we are ready to study the effect of dipolar interaction V_{dd}. In accordance with Ref. [16], we focus on a weak V_{dd} with $|D| \ll \omega l^3, gl^2$. We will show below that even a weak V_{dd} can dramatically change the stability of the sTG gas, and the key lies in the distinct spectral responses between different branches when V_{dd} is turned on.

Taking a typical g away from any g_c, in Fig. 3(a) we plot the energy shifts ΔE for the sTG gas and its nearest atom-dimer branch as varying $|D|$. Clearly, the atom-dimer energy changes rapidly as $|D|$ increases, while the sTG energy changes much more slowly. This can be attributed to very different real-space distributions of the two states. Namely, the atom-dimer is more localized along r, $r_+ \to 0$ and therefore it produces a significant spectral response to $V_{dd} \sim (1/|r|^3 + 1/|r_+|^3 + \cdots)$; on the contrary, the sTG gas is more extended and has little weight near r, $r_+ \to 0$, leading to a negligible energy shift. At small D, ΔE of each branch can be well approximated by mean-field shift $\langle V_{dd}\rangle$, as shown by dotted lines in Fig. 3(a). This allows us to analytically determine the shift of the crossing point, $\Delta(1/g_c)$, by equating (4) and (6) after adding up $\langle V_{dd}\rangle$ for each branch:

$$\Delta(1/g_c) = \frac{\langle V_{dd}\rangle_{ad} - \langle V_{dd}\rangle_{sTG}}{\partial E_d/\partial(1/g) - 3J/2}. \tag{7}$$

Equation (7) tells us that the distinct spectral responses, $\langle V_{dd}\rangle_{sTG} \neq \langle V_{dd}\rangle_{ad}$, directly lead to a finite shift $\Delta(1/g_c)$ of interbranch crossing. Moreover, the sign of $\Delta(1/g_c)$ exactly follows D: a positive D will drive the crossing point towards resonance [$\Delta(1/g_c) > 0$], while a negative D drives it oppositely [$\Delta(1/g_c) < 0$]. All of these features are verified numerically in Fig. 3(b), where Eq. (7) provides a reasonably good fit to the shift $\Delta(1/g_c)$ at small $|D|$. In addition, we observe that $\Delta(1/g_c)$ becomes less pronounced for crossings near resonance. This can be attributed to the large denominator of Eq. (7) produced by $\partial E_d/\partial(1/g) \propto g^3$ for deep dimers. Therefore, V_{dd} can only visibly affect the level crossings with small n but not those with large n near resonance.

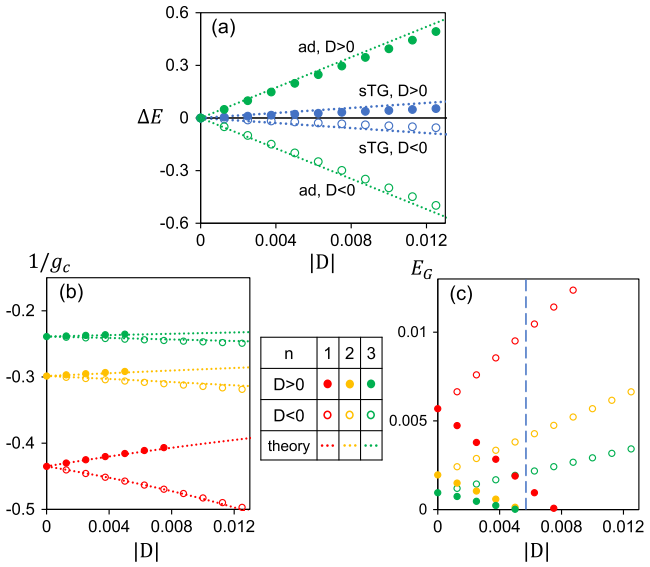

FIG. 3. Response of three fermions to a weak dipolar interaction with strength D. (a) Energy shifts of sTG and excited atom-dimer branches as functions of $|D|$ at given $\omega l/g = -0.27$. Dotted lines show mean-field shifts $\langle V_{dd}\rangle$. (b) Locations of three avoided crossings [as marked by "$n = 1, 2, 3$" in Fig. 2(a)] as functions of $|D|$. Dotted lines show linear fits according to Eq. (7). (c) Associated energy gap E_G of each avoided crossing as a function of $|D|$. Dotted vertical line marks the strength of repulsive D used in experiment [16]. Here the energy ΔE, coupling g, and dipolar force D are, respectively, in units of ω, ωl, and ωl^3.

Given the intimate relation between $1/g_c$ and E_G [see Figs. 2(e1) and 2(e2)], the shift of $1/g_c$ by V_{dd} inevitably leads to the change of E_G, as plotted in Fig. 3(c). For a repulsive $V_{dd}(D > 0)$, all $1/g_c$ shift toward resonance with decreasing E_G, indicating a more stable sTG gas; while for an attractive $V_{dd}(D < 0)$, $1/g_c$ shifts away from resonance with increasing E_G, indicating a less stable sTG gas. Again, E_G changes most visibly for the outmost crossing ("$n = 1$"). Remarkably, all E_G become vanishingly small at a weak $D/(\omega l^3) \sim 0.008$, suggesting an extremely sTG gas in the whole $g < 0$ regime. We note that if we take the same D as used in experiment [16], as marked by the vertical dotted line in Fig. 3(c), the outmost E_G ("$n = 1$") is greatly reduced compared to $D = 0$ case, and all other E_G decrease to $< 10^{-4}\omega$. Besides D, we have also checked the effect of the dipolar cutoff r_c. It is found that a smaller r_c one can generate more energies for the localized atom-dimer branch [21] and thus the change of $1/g_c$ and E_G will be more dramatic at the same D.

In the above we have shown how a weak repulsive or attractive V_{dd} can greatly affect the stability of fermionic

sTG gas, while leaving its energy essentially unchanged. We have checked that similar physics also hold for three identical bosons [21], including the distinct energy responses between sTG gas and excited bound states as well as the dependence of sTG stability on the sign of V_{dd}. Here a crucial difference from the fermion case is that the bosonic bound states are all cluster ones that no longer follow the atom-dimer description. Further, for a much larger bosonic system as in experiment [16], which is inaccessible by exact numerics, we expect the above loss mechanism to equally work. In this case, the sTG branch can also be well identified as the adiabatic extension of TG gas to the $1/g < 0$ side, and as changing $1/g$ there should be many more cluster bound states from higher harmonic levels to (avoided) level cross with it. However, only those far from resonance are responsible for the instability of the sTG gas due to their stronger hybridizations in between. Similar to the few-body case, a weak dipolar force is expected to shift these bound state spectra visibly due to their localized nature but can hardly affect the energy of the sTG branch. Again, this leads to a significant change of sTG stability that is sensitive to the sign of V_{dd} (see Fig. 1).

In summary, we have revealed the underlying mechanism for a mysterious phenomenon recently observed in 1D sTG gas, namely, its greatly enhanced (reduced) stability by a weak repulsive (or attractive) dipolar interaction. The key to this phenomenon is the significant spectral response of excited bound states—the decay channel of sTG gas—to the dipolar force. Therefore the sTG gas is indirectly affected due to the interbranch hybridization at their level crossing, leading to a modification of sTG stability but not its energy. In this regard, our results suggest a powerful tool to tune the stability of the target state by manipulating its decay channel under designed potentials. Such state-selective manipulation may help one to engineer many more fascinating long-lived quantum states in a cold atoms platform in the future.

We thank Benjamin Lev for positive and helpful feedback on our manuscript. This work is supported by the National Natural Science Foundation of China (12074419, 12134015) and the Strategic Priority Research Program of Chinese Academy of Sciences (XDB33000000).

*xlcui@iphy.ac.cn

[1] G. E. Astrakharchik, J. Boronat, J. Casulleras, and S. Giorgini, Beyond the Tonks-Girardeau gas: Strongly correlated regime in quasi-one-dimensional Bose gases, Phys. Rev. Lett. **95**, 190407 (2005).

[2] M. T. Batchelor, M. Bortz, X. W. Guan, and N. Oelkers, Evidence for the super Tonks-Girardeau gas, J. Stat. Mech. (2005) L10001.

[3] E. Haller, M. Gustavsson, M. J. Mark, J. G. Danzl, R. Hart, G. Pupillo, and H.-C. Nägerl, Realization of an excited, strongly correlated quantum gas phase, Science **325**, 1224 (2009).

[4] L. Guan and S. Chen, Super-Tonks-Girardeau gas of spin-1/2 interacting fermions, Phys. Rev. Lett. **105**, 175301 (2010).

[5] G. Zürn, F. Serwane, T. Lompe, A. N. Wenz, M. G. Ries, J. E. Bohn, and S. Jochim, Fermionization of two distinguishable fermions, Phys. Rev. Lett. **108**, 075303 (2012).

[6] S. Murmann, F. Deuretzbacher, G. Zurn, J. Bjerlin, S. M. Reimann, L. Santos, T. Lompe, and S. Jochim, Antiferromagnetic Heisenberg spin chain of a few cold atoms in a one-dimensional trap, Phys. Rev. Lett. **115**, 215301 (2015).

[7] S. E. Gharashi and D. Blume, Correlations of the upper branch of 1D harmonically trapped two-component Fermi gases, Phys. Rev. Lett. **111**, 045302 (2013);

[8] P. O. Bugnion and G. J. Conduit, Ferromagnetic spin correlations in a few-fermion system, Phys. Rev. A **87**, 060502 (R) (2013);

[9] X. Cui and T.-L. Ho, Ground-state ferromagnetic transition in strongly repulsive one-dimensional Fermi gases, Phys. Rev. A **89**, 023611 (2014).

[10] E. J. Lindgren, J. Rotureau, C. Forssén, A. G. Volosniev, and N. T. Zinner, Fermionization of two-component few-fermion systems in a one-dimensional harmonic trap, New J. Phys. **16**, 063003 (2014).

[11] A. G. Volosniev, D. V. Fedorov, A. S. Jensen, M. Valiente, and N. T. Zinner, Strongly interacting confined quantum systems in one dimension, Nat. Commun. **5**, 5300 (2014).

[12] F. Deuretzbacher, D. Becker, J. Bjerlin, S. M. Reimann, and L. Santos, Quantum magnetism without lattices in strongly interacting one-dimensional spinor gases, Phys. Rev. A **90**, 013611 (2014).

[13] L. Yang, L. Guan, and H. Pu, Strongly interacting quantum gases in one-dimensional traps, Phys. Rev. A **91**, 043634 (2015).

[14] L. Yang and X. Cui, Effective spin-chain model for strongly interacting one-dimensional atomic gases with an arbitrary spin, Phys. Rev. A **93**, 013617 (2016).

[15] J. Levinsen, P. Massignan, G. M. Bruun, and M. M. Parish, Strong-coupling ansatz for the one-dimensional Fermi gas in a harmonic potential, Sci. Adv. **1**, e1500197 (2015).

[16] W. Kao, K.-Y. Li, K.-Y. Lin, S. Gopalakrishnan, and B. L. Lev, Topological pumping of a 1D dipolar gas into strongly correlated prethermal states, Science **371**, 296 (2021).

[17] T. Cheon and A. Tanaka, New anatomy of quantum holonomy, Europhys. Lett. **85**, 20001 (2009).

[18] S. Sinha and L. Santos, Cold dipolar gases in quasi-one-dimensional geometries, Phys. Rev. Lett. **99**, 140406 (2007).

[19] P. Giannakeas, V. S. Melezhik, and P. Schmelcher, Dipolar confinement-induced resonances of ultracold gases in waveguides, Phys. Rev. Lett. **111**, 183201 (2013).

[20] L. Guan, X. Cui, R. Qi, and H. Zhai, Quasi-one-dimensional dipolar quantum gases, Phys. Rev. A **89**, 023604 (2014).

[21] See Supplemental Materials at http://link.aps.org/supplemental/10.1103/PhysRevLett.131.203002 for more details on the exact solutions of three-body problems, the wavefunction and energy of sTG gas and the numerical results of three identical bosons.

[22] S. E. Gharashi, K. M. Daily, and D. Blume, Three s-wave-interacting fermions under anisotropic harmonic confinement: Dimensional crossover of energetics and virial coefficients, Phys. Rev. A **86**, 042702 (2012).
[23] Pino D'Amico and M. Rontani, Three interacting atoms in a one-dimensional trap: A benchmark system for computational approaches, J. Phys. B **47**, 065303 (2014).
[24] E. Haller, M. J. Mark, R. Hart, J. G. Danzl, L. Reichsöllner, V. Melezhik, P. Schmelcher, and H.-C. Nägerl, Confinement-induced resonances in low-dimensional quantum systems, Phys. Rev. Lett. **104**, 153203 (2010).
[25] S. Sala, P.-I. Schneider, and A. Saenz, Inelastic confinement-induced resonances in low-dimensional quantum systems, Phys. Rev. Lett. **109**, 073201 (2012).
[26] S. Sala, G. Zürn, T. Lompe, A. N. Wenz, S. Murmann, F. Serwane, S. Jochim, and A. Saenz, Coherent molecule formation in anharmonic potentials near confinement-induced resonances, Phys. Rev. Lett. **110**, 203202 (2013).